Scripta Materialia 171 (2019) 36–41

Contents lists available at ScienceDirect

Scripta Materialia

journal homepage: www.elsevier.com/locate/scriptamat

Slip and fracture behavior of δ-Ni_3Nb plates in a polycrystalline nickel-based superalloy during fatigue

Yun Wu [a], Shuangming Li [b], Maodong Kang [a,*], Yunting Li [c], Yahui Liu [a], Haiyan Gao [a], Baode Sun [a,d], Jun Wang [a,d,**]

[a] School of Materials Science and Engineering, Shanghai Jiao Tong University, Shanghai 200240, PR China
[b] State Key Laboratory of Solidification Processing, Northwestern Polytechnical University, Xi'an 710072, PR China
[c] Instrumental Analysis Center, Shanghai Jiao Tong University, Shanghai 200240, PR China
[d] Shanghai Key Laboratory of Advanced High-temperature Materials and Precision Forming, Shanghai Jiao Tong University, Shanghai 200240, PR China

ARTICLE INFO

Article history:
Received 10 April 2019
Received in revised form 8 June 2019
Accepted 8 June 2019
Available online 26 June 2019

Keywords:
δ-Ni_3Nb
Fatigue
Slip
Fracture
Crystal structure

ABSTRACT

The fatigue deformation behavior of δ-Ni_3Nb (DO_a intermetallic phase in nickel-based superalloy) was analyzed in detail to determine its fracture characteristics and possible slip systems. Strong arrangement-dependence (i.e. arrangement direction of plate length relative to loading direction) deformation characteristics were observed. When δ plates were arranged not paralleling to the loading direction, they exhibited certain degree of fatigue resistance. Slip traces were found in the non-parallel δ plates after some fatigue cycles. By analyzing the traces and habit plane of δ, the possible operative slip systems were confirmed to be $(010)_\delta[100]_\delta$ and $(010)_\delta[102]_\delta$.

The strong requirement of improving the reliability of aero-engine components promotes a great deal of microstructure relative researches of fatigue performance, aiming to well understand the fatigue fracture behavior of candidate materials [1–5]. Among these studies, second-phase particles in the widely used IN718 polycrystalline nickel-based superalloy have attracted intensive interests because their crystal structures and deformation characteristics are quite different from the alloy matrix [6–8]. The major and minor strengthening phases in IN718, namely γ″-Ni_3Nb (DO_{22}) and γ′-$Ni_3(Al,Ti)$ ($L1_2$) respectively, have been extensively researched, because they are vital to the high mechanical properties [9–11]. Also, as a common and stable phase in IN718, δ-Ni_3Nb has been widely studied to understand its precipitation behavior and effects on mechanical properties [1,12]. Generally, δ has the solvus temperature between 990 °C and 1020 °C and can start to precipitate at ~1000 °C for short times (below 1 h) [13,14]. This indicates that δ cannot be ignored in studying the plastic deformation and fracture of IN718. The precipitation of granular δ at grain boundary is believed to provide strong pinning effect on grain growth and thusly improve fatigue resistance and stress rupture property [8,12,15]. Unlike this, plate-like δ particles provide certain fatigue resistance to the matrix by hindering dislocation glide [9]. The past works have provided excellent findings about the correlation between δ and fatigue property, but the detailed experimental results about the fatigue deformation and fracture behavior of δ have been still rather limited. Although the fatigue fracture of IN718 mainly originate from surface defect, surface strain localization grain and surface inclusion, the deformation and fracture of precipitates may also cause internal microcracks and accelerate crack propagation [1,16]. Therefore, it is necessary to scrutinize the fatigue deformation and fracture characteristics of δ phases.

Generally, δ has an orthorhombic DO_a structure [12], which is thought to be derived from the hexagonal close packed structure, such as DO_{19} [17,18]. The δ phases have an epitaxial relation with the γ-Ni matrix: $\{111\}_\gamma//(010)_\delta$ and $\langle 1\bar{1}0\rangle_\gamma//[100]_\delta$ [15,17,19]. Apparently, the habit plane of δ is the close packed $\{111\}_\gamma$ and $(010)_\delta$ planes [17]. In addition to γ, δ should also be associated with γ″, since the metastable γ″ can transform into stable δ during long-term aging or service. By combining crystallographic and high resolution transmission electron microscopy (HRTEM) analyses, the transformation of γ″ → δ is confirmed to be a purely geometrical

* Corresponding author.
** Correspondence to: J. Wang, Shanghai Key Laboratory of Advanced High-temperature Materials and Precision Forming, Shanghai Jiao Tong University, Shanghai 200240, PR China.
E-mail addresses: kangmd518@sjtu.edu.cn (M. Kang), junwang@sjtu.edu.cn (J. Wang).

https://doi.org/10.1016/j.scriptamat.2019.06.013
1359-6462/

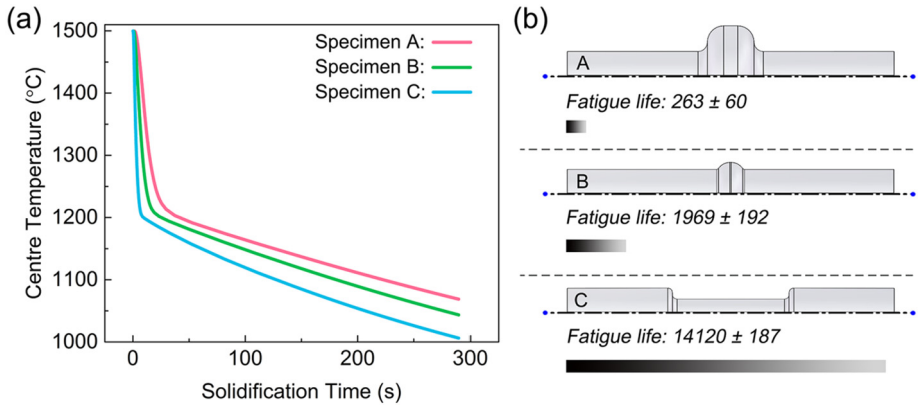

Fig. 1. (a) Simulated results of the temperature at the center of the specimen varying with solidification time. (b) Axisymmetric diagrams of three casting specimens and their respective fatigue life.

modification of the compact planes stacking sequence, i.e. the unique Burgers vector $1/6[\overline{1}\overline{1}1]_{\gamma'}$ on the compact plane $(112)_{\gamma'}$ is available to create a low energy stacking fault, corresponding to the transformation of $D0_{22}$ stacking sequence to locally $D0_a$ structure [17,19]. As to the plastic deformation characteristics of δ, some outstanding results have been made in studying its single crystal deformation. The operative slip systems of δ single crystal have been determined: (010)[100], (001)[100], $\{201\}\langle 10\overline{2}\rangle$ and (010)[001] depending on its crystal orientation relative to loading direction (LD) [18,20]. However, these results have not yet been applied to the analysis of δ phases within IN718. When IN718 is subjected to macroscopic load, the plastic deformation of γ matrix and γ″ would inevitably affects the accompanied δ due to the above mentioned epitaxial relations and strain localization within γ matrix [2,17]. Moreover, because each of the four habit $\{111\}_\gamma$ planes has three close packed directions, twelve variants of δ can form within the γ matrix. And δ particles could act as nuclei for another δ variant by dissociation of dislocations on the conjugate plane [12]. Therefore, δ plates show obvious intersecting arrangement configuration. The anisotropy and intersection of δ determines that the deformation behavior of different arrangement configurations (e.g. angle of its length direction relative to LD) should be various [8,12]. In the present study, new attempts are made to explore the evolution of δ particle under fatigue load. Emphasis will be placed on analyzing the deformation and fracture behavior of the particle in different orientations. Through these results, the possible operative slip systems and arrangement dependent fracture characteristics of δ particle in IN718 have been proposed.

Polycrystalline IN718, with a nominal composition of 19% Cr, 18.55% Fe, 3% Mo, 5% (Nb + Ta), 0.9% Ti, 0.5% Al, 0.05% C (mass%), is chosen as master alloy to manufacture casting bars using investment casting process [21]. Three kinds of bars with expected different fatigue lives were designed based on solidification rate [22]. The variation of temperature in their central positions with solidification time was simulated by COMSOL Multiphysics software (Fig. 1a). The heat transfer coefficient and thermal conductivity data were taken from the literature [23] and software, respectively. To eliminate the microsegregation and precipitate hardening phases, standard heat treatments (ST) were performed in air following the regimes of 1095 °C × 1 h/air cooling + 955 °C × 1 h/air cooling + 720 °C × 8 h/furnace cooling in rate of 56 °C/h + 620 °C × 8 h/air cooling to room temperature [9]. The detailed metallurgical/precipitation state of the material after ST is available in Supplementary materials 1.1. Fatigue tests were performed to the cylindrical specimens (with the gauge dimensions of approximately Ø6 × 15 mm) at room temperature using uniaxial and push-pull mode on a computer-controlled hydraulic machine. The other testing parameters are constant stress amplitude ($\sigma_m = 380$ MPa), stress ratio ($R = -1$) and triangular wave (frequency = 0.3 Hz). The fatigue life of each specimen is shown in Fig. 1b, which is consistent with our inference. Selective etching technique was adopted to remove the matrix and expose δ in longitudinal section samples. Before selective etching, it is necessary to do some surface treatments on the desired surface to eliminate the surface stress layer. The surface treatments adopted were electrolytic polishing (20% H_2SO_4 + 80% CH_3OH, at the voltage of 20 V for 20 s) and vibration polishing (using silica suspension for 2 h). Subsequently, electrolytic etching (15 g Cr_2O_3 + 10 ml H_2SO_4 + 150 ml H_3PO_4, at the voltage of 5 V for 60 s) was used for removing matrix. The etched surface was observed by TESCAN MIRA3 field emission scanning electron microscopy (SEM). Focused ion beam (FIB, TESCAN GAIA3) technique was used to sectioning the δ plate with particular arrangement. The transmission Kikuchi diffraction (TKD) technique was performed to analyze local misorientation (LMO) within γ matrix of the FIB sample by using the same SEM instrument and associated AZtec Nordlys Max^3 electron backscatter diffraction (EBSD) detector at step size ~50 nm and voltage ~20 kV. In addition, the morphologies and crystal orientation of δ were analyzed by JEOL 2100F field emission transmission electron microscopy (TEM) by using thin foils and FIB sample.

Fig. 2a shows the typical plate-like δ particles and three directions of δ plates, namely length, width and thickness. Fig. 2b shows the TEM bright-field micrograph and selective area electron diffraction (SAED) patterns of γ and δ. Then, the crystal orientation relationship between γ and δ can be obtained as following: $(1\overline{1}\overline{1})_\gamma//(0\overline{2}0)_\delta$ and $[01\overline{1}]_\gamma//[100]_\delta$. Fig. 2c schematically shows the lattice arrangement of the two oriented planes. Fig. 2d shows the typical fracture surface containing fractured δ plates, indicating their fracture along fatigue striations within matrix, rather than debonding.

It should be noted that the strain localization within slip bands and near twin boundaries (TBs) in the γ matrix is a key factor determining fatigue fracture [2]. So, before discussing the fatigue deformation mechanism of δ, the slip and twinning behavior of γ matrix are firstly addressed here. It was stated that, for a polycrystalline and twinned IN718 alloy, strain localization first develops in the vicinity of and parallel to TBs below the 0.2% yield strength due to elastic strain mismatch and/or high Schmid factor of the active slip system ($\{111\}\langle 1\overline{1}0\rangle$), while above the 0.2% yield strength, transgranular slip localization is the dominant plastic mechanism at room temperature (active slip system $\{111\}\langle 1\overline{1}0\rangle$) [2]. And different slip systems can be active at the same slip band depending on the macroscopic stress level [2]. In the present study, the grain size of present casting is much larger than that of forging state and no TB can be found. So it is hard to figure out the exact slip system in local area. But the slip plane can be confirmed to be $\{111\}_\gamma$ [2,3]. Since $\{111\}_\gamma$ is the habit plane of δ, the slip and strain localization

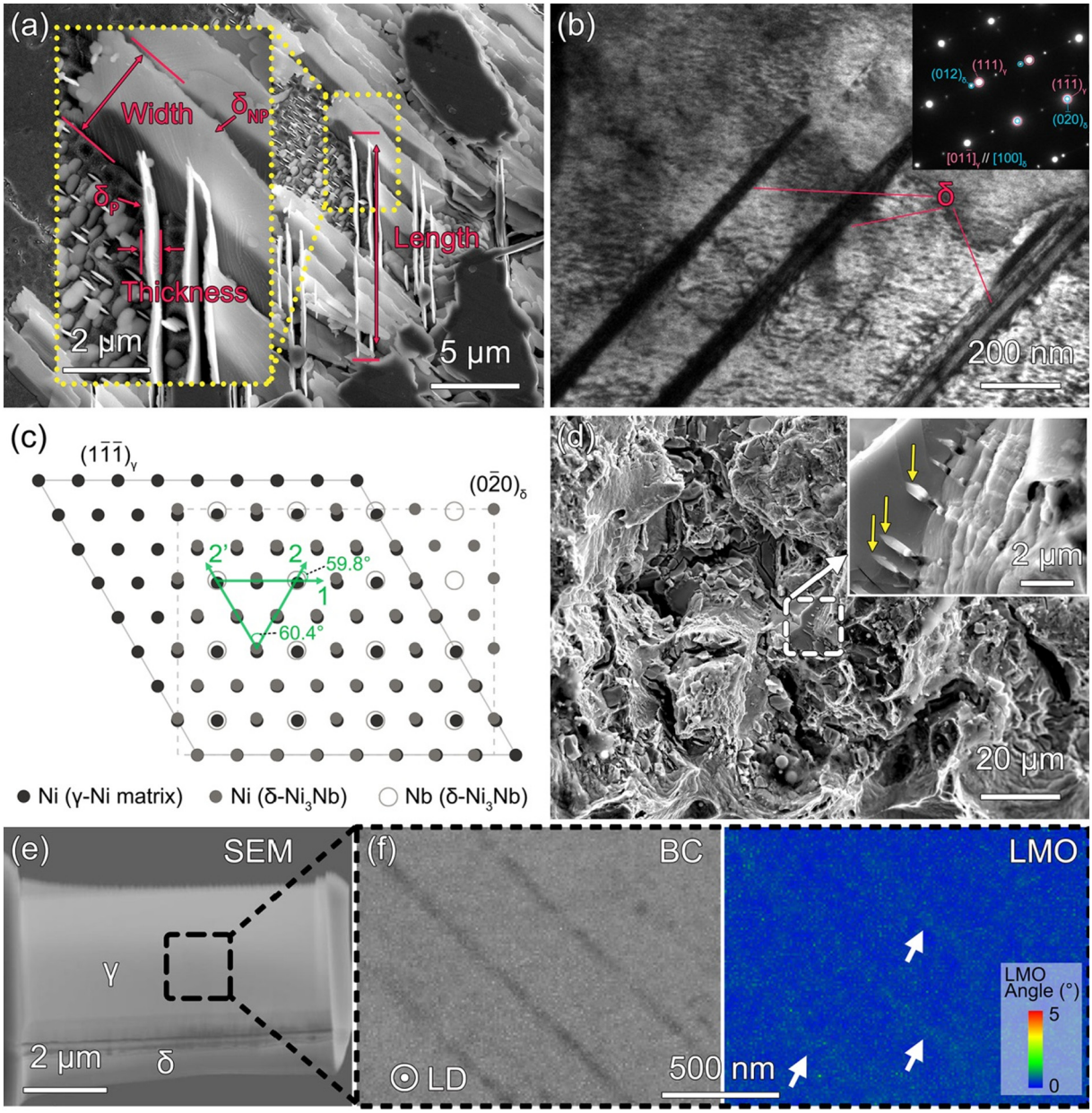

Fig. 2. (a) SEM image of the plate-like δ phases. (b) TEM bright-field image of the δ phases embedded within the γ matrix and their SAED patterns. (c) Schematic diagram of the orientation crystal planes of γ and δ. (d) SEM image of the fracture surface of specimen C shows the fractured δ plates (as highlighted by the yellow arrows). (e) SEM image of the FIB sample shows two parts, namely γ and δ, respectively. (f) Band contrast (BC) and LMO images obtained by analyzing the area indicated in (e) using TKD technique.

were carefully considered. Through FIB and EBSD techniques, some slip traces within γ matrix were observed near a δ plate (Fig. 2e and f). The LMO distribution indicates that strain localization indeed occur around slip bands [24]. More detailed description is available in Supplementary materials 1.2.

To accurately discuss the fatigue deformation of δ, two representative distributions are considered: i) LD approximately paralleling to length direction (Fig. 2a, denoted as δ_P); ii) LD non paralleling to length direction and the load acts directly on the width plane of δ (Fig. 2a, denoted as δ_{NP}). In short-term fatigue, the morphology of δ_{NP} shows no special characteristic (Fig. 3a). When the fatigue cycle increases, slip trace appears gradually, as indicated by the blue arrows in Fig. 3b. With the further increase of fatigue cycle, the number of slip traces increases significantly (Fig. 3c). Apparently, the fatigue deformation of δ_{NP} requires an incubation period. Only after enough cycles, the accumulated slip deformation and strain localization of matrix reaches a certain degree, and then the slip of δ_{NP} particle occurs [25]. It can also be seen from Fig. 3c that the slip traces in a single δ_{NP} particle have the characteristics of parallel arrangement, indicating the slipping preferentially along a specific crystal direction. In terms of the δ_P particle, the characteristics of branch cracking were observed in all the samples, indicating poor plastic deformation ability [8]. According to crystal growth characteristics and the crystal orientation relation between γ and δ, the width plane of δ_{NP} plate can be reasonably inferred as $(010)_\delta$ [15,26], which is the closest packed plane and possible slip plane of δ-Ni_3Nb crystal [26,27]. Without considering the existing mobile dislocation, sufficient resolved shear stress (τ) along the slip direction is needed to make

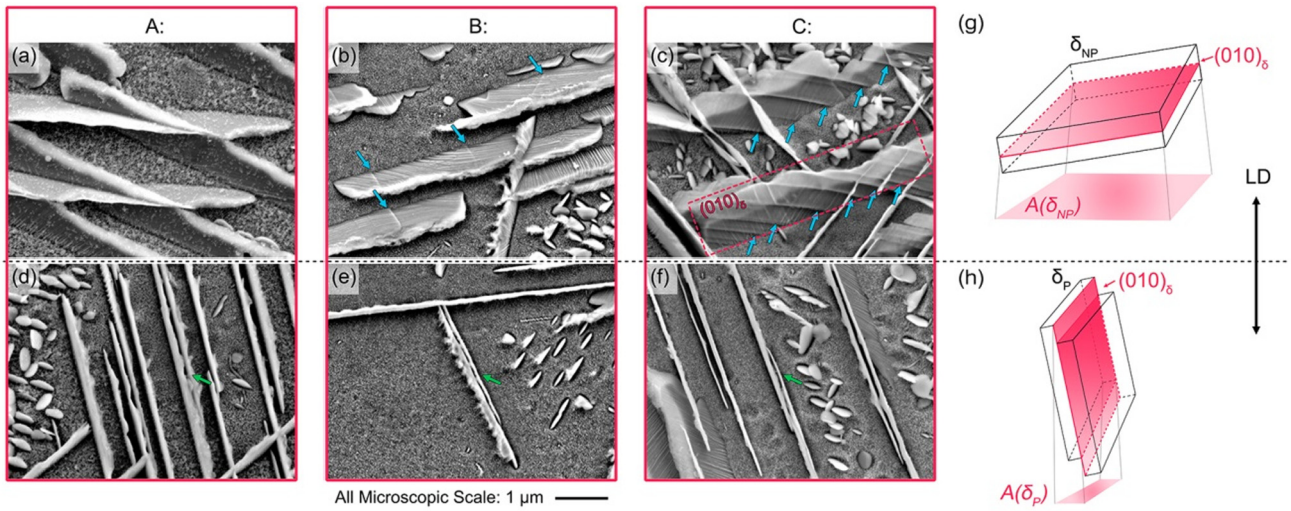

Fig. 3. SEM images show the morphologies of as-fatigued δ_{NP} particles (a)–(c) and δ_P particles (d)–(f) in specimen A, B and C, respectively. (g) Schematic diagram of the orientation crystal planes of γ and δ. Schematic diagrams show the stress state of habit plane of δ_{NP} (g) and δ_P (h).

the slip plane move. Generally, τ is proportional to the component of external force along the slip direction (Fs) and inversely proportional to the projection area of slip plane along the force direction (A). Here we assume that Fs is equal in two loading cases (Fig. 3g and h). Obviously, $A(\delta_P)$ is much smaller than $A(\delta_{NP})$, indicating that δ_{NP} particle has lower τ and better ability to resist fatigue fracture.

In addition to slip, fracture of δ_{NP} particle was also observed in the long-term fatigue specimen. Two fractured δ_{NP} particles after long-term fatigue were observed in C specimen (Fig. 4a and b). The δ_{NP} particle in Fig. 4a exhibits not only cracking, but also obvious bending, showing a certain degree of ductility. Fig. 4b shows slip-induced fracture of a δ_{NP} particle. The multiple slip traces observed on particle surface indicates that the δ_{NP} can slip along multiple crystal directions. As mentioned above, δ crystal grows along $(010)_\delta$ plane and its width plane can be represented by $(010)_\delta$ [28]. Because the slip lines intersect (Fig. 4b), we can measure the angles and compare it with the angles of the crystal direction in the ideal close packed plane $(010)_\delta$ to determine the direction of the slip. The experimental angle between slip lines (a1 to a5 in Fig. 4b) is measured to be 58.9° ± 2.8°, which is in good agreement with the ideal crystal direction angles shown in Fig. 2c (crystal structure data from ICSD #108621) [27]. Thusly, the possible operative slip systems of δ can be inferred as: $(010)_\delta[100]_\delta$ and $(010)_\delta[102]_\delta$, in which the former is consistent with the previous studies [18,20].

Fig. 4c shows the different morphologies of two types of δ configurations in specimen C, i.e. branch cracking (yellow square) and plastic shearing (white square). As discussed above, the δ_P plates are hardly to slip on its close packed planes. The branch cracking characteristics of δ_P plates indicate that plastic deformation is hard to occur. The HRTEM observation of a δ_P plate (Fig. 4e) proves this opinion, since almost no dislocation or any other deformation structure presents in the plate. Conversely, the δ_{NP} plates show obvious plastic deformation traces (Fig. 4d). The HRTEM observation (Fig. 4f) of the δ_{NP} plate (Fig. 2e) indicates that several edge dislocations appear on $(020)_\delta$ plane, which again proves that $(010)_\delta$ is the possible slip plane. In this study, the interaction between dislocations and δ plates is not obvious. It may be ascribed to the low macroscopic stress, which makes the γ″ particles exhibit enough cyclic softening ability [1]. Then, the slip or shearing of δ plates in non-parallel configuration is reasonably inferred to be probably originated from the inside of the plates.

Furthermore, the δ and γ″ contents are also considered. Because of the similar chemical compositions and purely geometric transformation mechanism, the δ and γ″ contents are reasonably believed to have approximate inverse relation [1,17]. A recent study has demonstrated that a low δ/γ″ content ratio is responsible for the short fatigue life due relatively low stress relaxation effect under high γ″-content condition [1,19]. In the present study, statistic results show that the δ contents are 3.5% ± 0.6%, 7.2% ± 0.3% and 10.0% ± 0.8% for specimen A, B and C, respectively. Apparently, a roughly positive correlation between δ content and fatigue life can be established, which is consistent with the literature [1]. Detailed description is available in Supplementary materials 1.3.

In summary, the fatigue deformation and fracture characteristics of δ-Ni_3Nb phases at room temperature were investigated by surface treatment and electron microscopy methods. The response of δ to fatigue load is related to its arrangement relative to loading direction. The δ_P plates are prone to occur branch cracking and show no slip trace within the plates. Conversely, δ_{NP} particles exhibit a certain resistance to fatigue fracture. The fatigue deformation and slip of δ_{NP} particles need a certain incubation period. With the increase of fatigue cycles, the slip deformation of δ_{NP} particles gradually appears and ultimately evolves to bending and fracture. The possible slip systems of δ are proposed: $(010)_\delta[100]_\delta$ and $(010)_\delta[102]_\delta$.

Acknowledgements

The authors would like to appreciate the financial support for this work by National Key R&D Program of China, China (2016YFB0701405); Startup Fund for Youngman Research at SJTU, China (18X100040027); Aeronautical Science Foundation of China, China (2018ZE57012); and the State Key Laboratory of Solidification Processing in NWPU, China (SKLSP201852).

Appendix A. Supplementary material

Supplementary data to this article can be found online at https://doi.org/10.1016/j.scriptamat.2019.06.013.

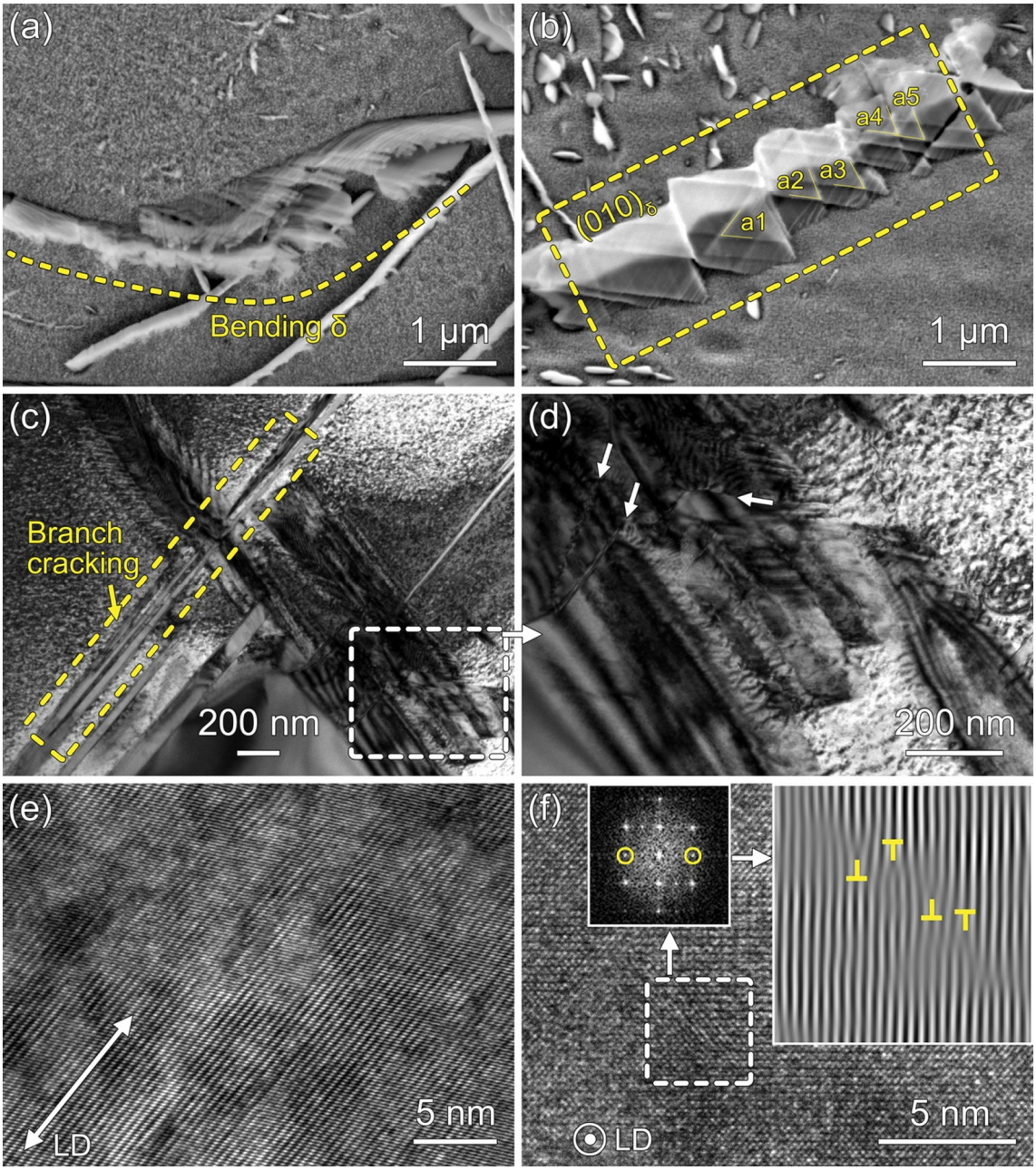

Fig. 4. (a)–(b) SEM images show the fractured δ_{NP} plates. (c) TEM bright-field image shows the as-fatigued morphologies of the two kinds of δ plates in specimen C. (d) A magnified TEM bright-field image shows the plastic deformation traces of the δ_{NP} plates indicated in (c). (e)–(f) HRTEM images taken along $[100]_{\delta}$ direction show the substructures within δ_P and δ_{NP} plates, respectively.

References

[1] D. Texier, A.C. Gómez, S. Pierret, J.M. Franchet, T.M. Pollock, P. Villechaise, J. Cormier, Metall. Mater. Trans. A 47 (2016) 1–14.
[2] J.H. Liu, N. Vanderesse, J.C. Stinville, T.M. Pollock, P. Bocher, D. Texier, Acta Mater. 169 (2019) 260–274.
[3] C.J. Boehlert, H. Li, L. Wang, B. Bartha, Adv. Mater. Process. 168 (2010) 41–45.
[4] S. Sui, J. Chen, E. Fan, H. Yang, X. Lin, W. Huang, Mater. Sci. Eng. A 695 (2017) 6–13.
[5] D.H. Jeong, M.J. Choi, M. Goto, H.C. Lee, S. Kim, Mater. Charact. 95 (2014) 232–244.
[6] K.N. Amato, S.M. Gaytan, L.E. Murr, E. Martinez, P.W. Shindo, J. Hernandez, S. Collins, F. Medina, Acta Mater. 60 (2012) 2229–2239.
[7] S. Sui, H. Tan, J. Chen, C. Zhong, Z. Li, W. Fan, A. Gasser, W. Huang, Acta Mater. 164 (2019) 413–427.
[8] H.Y. Zhang, S.H. Zhang, M. Cheng, Z.X. Li, Mater. Charact. 61 (2010) 49–53.
[9] J. Xu, Z. Huang, L. Jiang, Mater. Sci. Eng. A 690 (2017) 137–145.
[10] G.A. Rao, M. Kumar, M. Srinivas, D.S. Sarma, Mater. Sci. Eng. A 355 (2003) 114–125.
[11] C. Slama, M. Abdellaoui, J. Alloys Compd. 306 (2000) 277–284.
[12] S. Mahadevan, S. Nalawade, J.B. Singh, A. Verma, B. Paul, K. Ramaswamy, 7th International Symposium on Superalloy 718 and Derivatives, 2010 737–750.
[13] V. Beaubois, J. Huez, S. Coste, O. Brucelle, J. Lacaze, Mater. Sci. Technol. 20 (2013) 1019–1026.
[14] A. Niang, B. Viguier, J. Lacaze, Mater. Charact. 61 (2010) 525–534.
[15] M. Dehmas, J. Lacaze, A. Niang, B. Viguier, Adv. Mater. Sci. Eng. 2011 (2011) 1–9.
[16] Y. Yamashita, T. Murakami, R. Mihara, M. Okada, Y. Murakami, Int. J. Fatigue 117 (2018) 485–495.
[17] A. Niang, J. Huez, J. Lacaze, B. Viguier, Mater. Sci. Forum 636-637 (2010) 517–522.
[18] Y. Umakoshi, K. Hagihara, T. Nakano, Intermetallics 9 (2001) 955–961.
[19] D. Fournier, A. Pineau, Metall. Trans. A. 8 (1977) 1095–1105.
[20] K. Hagihara, T. Nakano, Y. Umakoshi, Acta Mater. 48 (2000) 1469–1480.

[21] S. Pattnaik, D.B. Karunakar, P.K. Jha, J. Mater. Process. Technol. 212 (2012) 2332–2348.
[22] M.C. Flemings, Solidification Processing, in: R.W. Cahn., P. Haasen., E.J. Kramer. (Eds.) Mater. Sci. Technol., Wiley-VCH Verlag GmbH & Co. KGaA, 2006.
[23] R.A. Overfelt, V. Sahai, Y.K. Ko, J.T. Berry, Superalloys 718, 625, 706, and Various Derivatives, 1994 189–200.
[24] J.C. Stinville, E. Martin, M. Karadge, S. Ismonov, M. Soare, T. Hanlon, S. Sundaram, M.L.P. Echlin, P.G. Callahan, W.C. Lenthe, Acta Mater. 152 (2018) 16–33.
[25] J.F. Nie, Scr. Mater. 48 (2003) 1009–1015.
[26] H. Sugimura, Y. Kaneno, T. Takasugi, Mater. Trans. 52 (2011) 663–671.
[27] P.M. Kelly, H.P. Ren, D. Qiu, M.X. Zhang, Acta Mater. 58 (2010) 3091–3095.
[28] D. Xu, D. Xue, J. Alloys Compd. 449 (2008) 353–356.